24th COBEM - 2017

24th ABCM International Congress of Mechanical Engineering
December 3-8, 2017, Curitiba, PR, Brazil

COBEM-2017-0645
IMPEDANCE CONTROL FOR ASSISTANCE IN CARGO HANDLING

Samuel Monteiro Junior
Sergio Delijaicov
Marko Ackermann
Fabrizio Leonardi
Centro Universitário FEI
Av. Humberto de Alencar Castelo Branco, 3972, São Bernardo do Campo, S.P., CEP: 09850-901
fabrizio@fei.edu.br, samuel_monteiro@terra.com.br, sergiode@fei.edu.br, mackermann@fei.edu.br

Abstract. *Power assisted systems can be used to overcome problems associated with manual cargo handling, such as injuries and muscle fatigue. This paper proposes the design of an impedance control system applied to a human-driven cargo cart by means of an electric motor to assist the operator. The control system aims at establishing the dynamic relationship between the applied force and the cart velocity, i.e. imposing a desired apparent mechanical impedance. The proposed methodology was inspired by the feedback linearization technique to promote an apparent change in mass and viscous friction coefficient of the system. It is shown that, with this technique, one can obtain an impedance control without the use of force sensors. For the experiments, a lab scale set of motor and tach generator is adopted. The controller requires information on angular velocity and acceleration, but only the velocity is measured directly, with a numerically estimated acceleration. The proposed control law generates additional terms in the differential equation to change system dynamics, also allowing compensation of Coulomb friction. To validate the results, a load cell was used which served to compare the prescribed impedance with the actual impedance of the system. In this validation process, it was observed that in all imposed impedance conditions whose control effort was below the actuator's saturation limit, the experimental impedance were very close to the prescribed impedance.*

Keywords: *Impedance control, DC motor, Robotics, Power assisted wheelchair*

1. INTRODUCTION

The human driving of cargo carts have very restricted performance that limits the speed of transport and payload. However, the use of an electric motor can replace or supplement the human force in the form of an assistance. The assistance can be pre-programmed or adapted to the operational condition and may have several characteristics, such as being a function of the floor slope.

Cuerva, Ackermann, and Leonardi (2016) compared three forms of assistance for power-assisted wheelchairs and concluded that the one in the form of impedance control has better performance in most of the maneuvers studied. In this work, it is argued that the assistance in the form of an apparent change of the total mass and other dynamic characteristics, such as damping, is also a convenient form of assistance for human-driven cargo transportation, since the operator takes part in the locomotion and perceives the assistance in a natural way.

An impedance control consists in making the dynamic relation between the applied force and the kinematics of the movement be maintained according to a reference impedance. Hogan (1985) was one of the first to report studies on mechanical impedance control. This type of control has been widely used in the robotic area whenever it is necessary to control the kinematics of a robot and there is an interaction with the environment or with human users (Jardim, *et al.*, 2009) and (Pedro, *et al.*, 2013). Other important applications for impedance control are those related to the rehabilitation area with applications in prostheses, orthoses and other means of mobility, which require complacent movements. Ibarra and Siqueira (2014) presented a review of the alternatives of impedance control strategies for application in robotic prostheses to perform therapies in patients with reduced mobility in the lower limbs.

Mehling and O 'Malley (2014) proposed the use of a model-type control structure as a way to obtain impedance control for systems with series elastic actuators (SEA). The authors show by means of numerical simulations that all coefficients of the desired impedance can be simultaneously changed at the price of an increase of the control effort to the same extent the desired impedance differs from the original impedance of the system.

In his work, Dellabianca *et al.*, 2013, found that 70% of wheelchair users suffer from problems such as chronic pain because they do not properly apply forces to propel the wheelchair or apply excessive forces (Sagawa *et al.*, 2012). A

natural solution to these problems is the use of power-assisted wheelchairs, the so-called PAPAW (Pushrim-Activated Power Assist Wheelchair). These chairs consist of electric motors that are normally driven by a request from the wheelchair-user by means of a contact on the pushrim of the wheel.

The work of Arva *et al.*, 2001, studied the mechanical efficiency of the wheelchairs and the quality of life of the users and verified that the users of assisted wheelchairs presented a lower rate of cardiac elevation due to the smaller force used and an increase in the mobility with better performances. Cooper *et al.*, 2002, studied the performance of a PAPAW thus determining its performance over that of manual chairs. Shibata and Murakami (2012) proposed an assisted control for an electric wheelchair that implements a complacent strategy of reaction forces. Cuerva, Ackermann and Leonardi (2016) compared three forms of assistance in wheelchair propulsion and concluded that the one in the form of impedance control has better performance in most of the maneuvers studied.

Popa and Liu (2001) implemented an impedance control in a hoist with a load capacity of 450 kg. The equipment is driven by human power, and therefore, depending on the load lifted, it can cause injuries to the operator. The longitudinal and transverse movements are made by the operator through the same cable that hoists the load. The authors treated the system equivalently to a pendulum and considered the force that generates the motion as a state variable of the model. In this way, it was possible to construct an observer to estimate that force. The proposed strategy makes the dynamic relationship between the estimated force and the velocity close to the desired impedance, i.e. desired apparent inertia and damping.

Electric assistance is also commonly used on bicycles. A controller drives the motor to assist the user while pedaling, saving efforts. Again, the impedance type assistance seems to be a suitable kind of assistance.

The present work aims to design and investigate the performance of the impedance control system of a power-assisted-human-driven cargo cart by means of an electric motor to assist the operator. The control system should promote an apparent change in mass, dynamic friction and the Coulomb friction. A controller is searched so that it does not require information of the force exerted by the operator, but only of the kinematics of the movement to make real applications feasible economically.

2. METHOD

2.1 Description of the test apparatus

The present research discusses the design of an impedance control system applied to a human-driven cargo cart by means of an electric motor to assist the operator. The experiment apparatus consist of an LJ Technical Systems that partially reproduces the characteristics of an electric cargo cart. It consists of a DC motor coupled to a DC tachogenerator on the same axis and strain sensors connected through a gear belts (1:9) forming a torque sensor for purposes of validation of the proposed control. The picture in Figure 1 shows the LJ system highlighting its electric motor and tachogenerator.

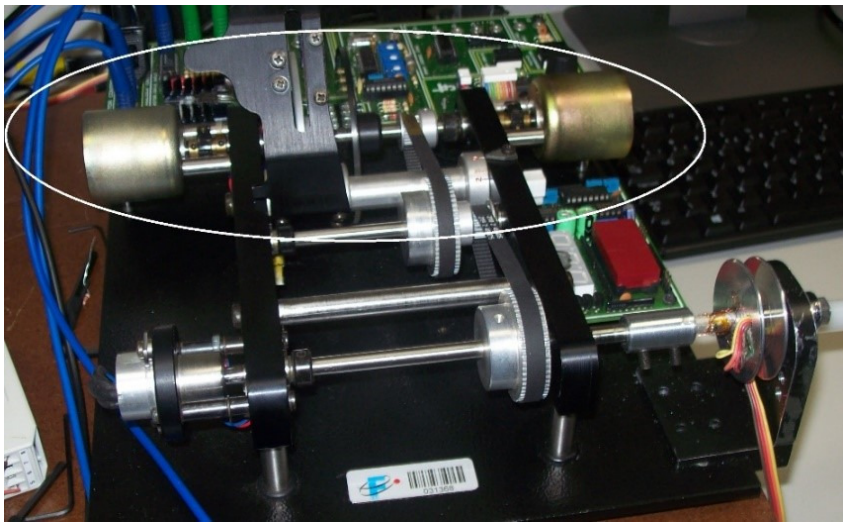

Figure 1. DC motor and tachogenerator.

It is assumed that the torque applied to the shaft can analogyly represent the force that is applied to the cargo cart by the user. An HBM RM 4220 amplifier is used to amplify the load cell signal. The pic of Figure 2 shows the axis, crank, and strain gauges that measure the torque produced by the user. Indeed, the proposed impedance control strategy does not require force measurement, but it is used in the impedance controller validation process.

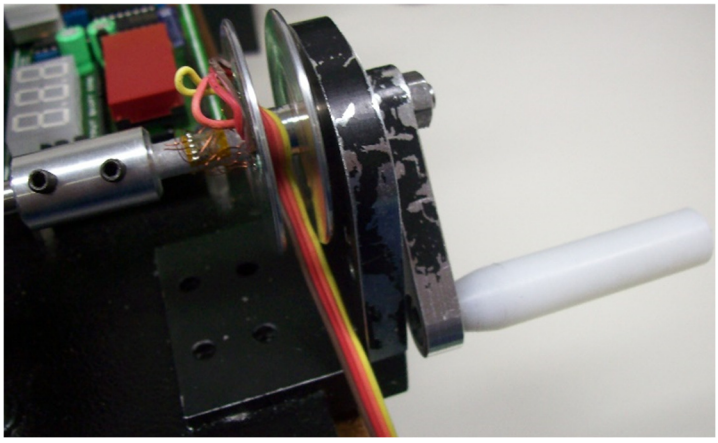

Figure 2. Load cell.

We used the Simulink™ operating it in real time for the numerical processing. The load cell signal is acquired by the Simulink via the NI-6221 data acquisition board from National Instruments and Matlab's Simulink Desktop Real Time toolbox. The angular velocity information on the load axis, as measured by the tachogenerator, is also sent to Simulink for the synthesis of the impedance control law. This control law also uses acceleration information, but this signal is not measured directly but estimated by numerical differentiation of the velocity signal.

2.2 Model

In his research, we investigate by means of simulation and also experimentally some advantages of the apparent change in the mass, viscous friction and in the Coulomb friction of the system.
For the design of the control system it is necessary to know the model of the electromechanical system formed by the cart-motor set. Thus, consider an electromechanical system consisting of a DC servo with a negligible inductance. An approximate model of this system is represented by the block diagram of Figure 3, where V_a is the armature voltage, T_l is the load torque, T_{at} is the friction Coulomb torque, ω is the angular velocity of the rotor, V_t is the voltage of the tachogenerator. The parameters R_a, J, B, and K_m represent the armature resistance, the moment of inertia, the dynamic friction and the torque constant of the motor, respectively

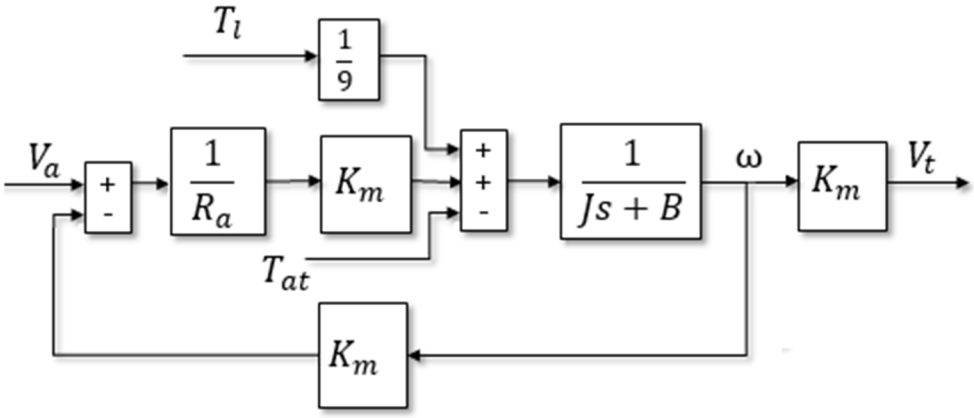

Figure 3. Block diagram of the electromechanical system.

The block diagram of Figure 3 can be represented equivalently by the differential equation

$$k(V_a + T_l\,\alpha - \eta) - \lambda\omega(t) = \dot{\omega}(t) \tag{1}$$

where λ is the total viscous friction and η the Coulomb friction of the system.

The parameters of the model were determined through practical experiments. Using (1) and an experiment without external torque, we can determine the time constant $\tau = 1/\lambda$ from the system response to a step-like excitation. Two constant voltages were imposed at different times and the transient response of the velocity ω was measured. From the

generated plot, the value corresponding to 63% of the steady velocity was used to determine the corresponding time elapsed since the application of the step-type signal. This duration is numerically equal to the time constant $\tau = 1/\lambda$.

With the system at the steady-state and without the external torque, the equation (1) becomes

$$\lambda\omega(\mathrm{t}) + \mathrm{k}\eta = V_a(t)k \tag{2}$$

By replacing the steady-state values of the two voltages and the two velocities in (2), and subtracting one equation from the other, it is possible to determine the parameter k

$$\lambda\frac{(\omega_2 - \omega_1)}{(V_{a2} - V_{a1})} = k \tag{3}$$

With the values of λ and k and with the steady-state values of V_a and ω, we get the value of η from (2).

The value of the ratio $\frac{K_m}{R_a}$ is obtained by means of a dynamometer, i.e. a load cell connected to the motor shaft. The motor shaft is held immobile while a known constant voltage is applied to the DC motor armature. In this conditions we can write

$$T_{Cell} = \frac{K_m}{R_a}V_a \tag{4}$$

where T_{Cell} is the torque measured by the load cell.

For the determination of the motor constant K_m, the voltage generated by the tachogenerator is used. Lenz's law gives the voltage generated by the tachogenerator in open circuit as

$$K_m = \frac{V_a(t)}{\omega(t)} \tag{5}$$

Although (5) is worth for any speed $\omega(t)$, a constant velocity imposed by a constant voltage applied to the motor is used. The voltage V_a is measured directly at the terminals of the tachogenerator and the velocity is measured by means of an optical sensor present in the system LJ. With the frequency of the pulses of the optical sensor, the velocity ω is obtained.

Finally, we get the moment of inertia

$$J = \frac{K_m}{R_a k} \tag{6}$$

and the parameter

$$\alpha = \frac{R_a}{K_m} \tag{7}$$

2.3 Control Strategy

Inspired on the work of Cuerva, Ackermann and Leonardi (2016), at least three control strategies can be considered in this cargo handling assistance.

A first strategy is one that does not either require the use of sensors of force or the kinematics. An input signal indicates if operator is in contact with the cargo cart, thus enabling the assistance. In practice, an on-off type switch typically does switching of this assistance. The system is subject to the torque that the operator applies, plus a torque imposed by the motor. In this type of strategy, we tipically tend to choose a high value of assistance in such a way that the operator makes

only minor adjustments in the conduction of the system. In this scenario, the operator makes a minimal effort, but typically loses the sensitivity of the movement.

The second strategy considered requires a sensor of the force applied by the operator, since the strategy is based on the amplification of the force applied. The control law of this strategy is given by

$$V_a(t) = \beta T_l(t), \tag{8}$$

where β is a positive and adjustable gain. With this control law the system is described by

$$(T_l + \beta T_l(t) - \eta sign(\omega))k = \dot{\omega}(t) + \lambda\omega(t) \tag{9}$$

It should be noted in (9) that this assistance strategy may be more adequate than the previous because it allows for the change of the apparent impedance of the system. However, both the moment of inertia and the damping coefficient are changed in the same ratio, implying that the time constant cannot be changed. That is, the dynamic characteristic of the system, in fact, is not changed, but only its gain.

The third strategy, the one proposed in this work, allows making the apparent change of the inertia, viscous friction and the Coulomb friction of the system, all independently. This strategy is based on an impedance control by direct model matching through the feedback of the kinematic variables. To analyze this strategy it is convenient to rewrite (1) as

$$\frac{K_m}{R_a}(V_a + T_l\alpha - \eta) - C\omega(t) = J\dot{\omega}(t) \tag{10}$$

where $C = J\lambda$ is the global coefficient of viscous friction and J is the moment of inertia of the system.

With the impedance control, the armature voltage V_a is used to transform the model (10) into the system described by

$$(J - J_1)\dot{\omega}(t) + (C - C_1)\omega(t) = \frac{K_m}{R_a}\left(T_l\alpha - (\eta - \eta_1)\right) \tag{11}$$

where J_1, C_1, η_1 represent the changes of moment of inertia, coefficient of viscous friction and the friction of Coulomb, respectively.

The control law that leads from (10) to (11) was inspired by the calculated torque control technique (Slotine, 1991) and chosen because it is not necessary to use force sensors and it is given by

$$V_a(t) = \frac{R_a}{K_m}(J_1\dot{\omega}(t) + C_1\omega(t) + \frac{K_m}{R_a}\eta_1) \tag{12}$$

That is, the operator, when applying a force, perceives the apparent moment of inertia $(J - J_1)$, the coefficient of apparent viscous friction $(C - C_1)$, and the apparent Coulomb friction $(\eta - \eta_1)$. It should be noted that the control law (12) requires the instantaneous information of the angular velocity $\omega(t)$ and the angular acceleration $\dot{\omega}(t)$.

3. RESULT

The real-time implementation of the mechanical impedance control and external torque measurement law was done using the Simulink Desktop Real Time through the National Instruments NI-6221 DAC board.

Table 1 contains the values of the estimated parameters, according to the procedure described in the previous section.

Table 1. Estimated plant parameters

K_m	0.0171	$N = m/W^2$
K_m / R_a	$1.2185\ 10^{-2}$	Nm/V
J	$4.933\ 10^{-5}$	kgm^2
η	0.4397	Nm
λ	4.153	s^{-1}
C	$2.05\ 10^{-5}$	$Nm.s$

With the application of the control law (12) the changes imposed on J and C are investigated. Eight simulations were made, and the desired value of J , C and η were changed according to Table 2

Table 2. Simulation data

J				
original	+25%	-25%	+50%	-50%
4.93E-05	6.17E-05	3.70E-05	7.40E-05	2.47E-05
C				
original	+25%	-25%	+50%	-50%
4.153	5.191	3.115	6.229	2.076
η				
original	+100%	-100%	+50%	-50%
0.4397	0.0	0.8793	0.2198	0.6595

The tests evaluate the consequences of the change of impedance parameters in the velocity response signal when the external torque is a step-type signal generated by a voltage applied to the input of the LJ system, equivalent to a real external torque. The signal used comprises a set of steps with different amplitudes, so that it was possible to observe how the alteration of the parameters influences the system response, both in acceleration and in deceleration. The first step has an amplitude of 0.27 Nm, applied at the instant 0.5 s of the simulation, which is then reduced to 0.16 Nm. The plot of Figure 4 illustrates the torque signal used in the tests.

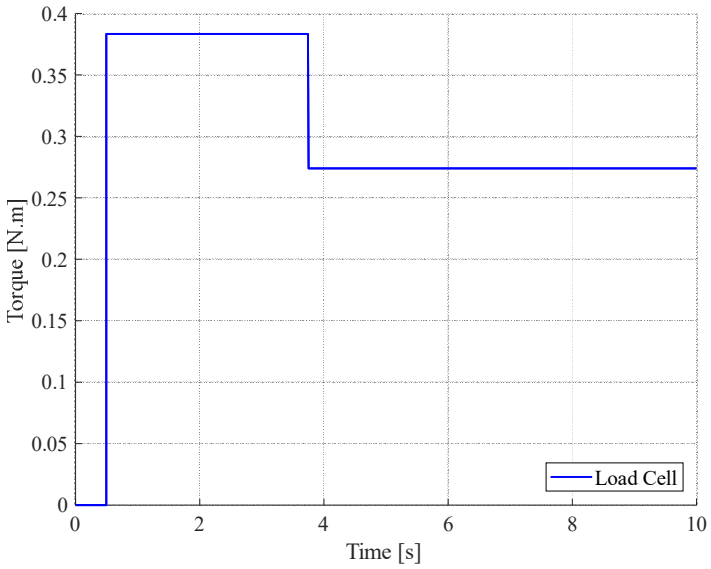

Figure 4. External torque applied to the system similar to torque applied by the operator.

For illustration purposes, consider in the following the detailing of one of the experiments performed.

With the apparent modification of the viscous friction, the system presents a corresponding variation in the time constant and the final value of the response, both caused by the gain change (see Figure 5). After 7.5 s, a 100% Coulomb

friction compensation was inserted and a corresponding change in the final value of the response was observed proportional to the changed parameter. When a 25% increase in the viscous friction coefficient is imposed, the system shows a lower time constant and a steady-state of amplitude smaller than the original system (lower gain). It should be noted that, in this case, the control effort presented a transient and a steady-state lower when compared to the original system. When a 25% decrease in the viscous friction coefficient is imposed, the system shows a longer time constant and a steady state of amplitude larger than the original system (higher gain). In this case, the control effort presented a transient and a steady-state higher when compared with the original system, even with the Coulomb friction compensation.

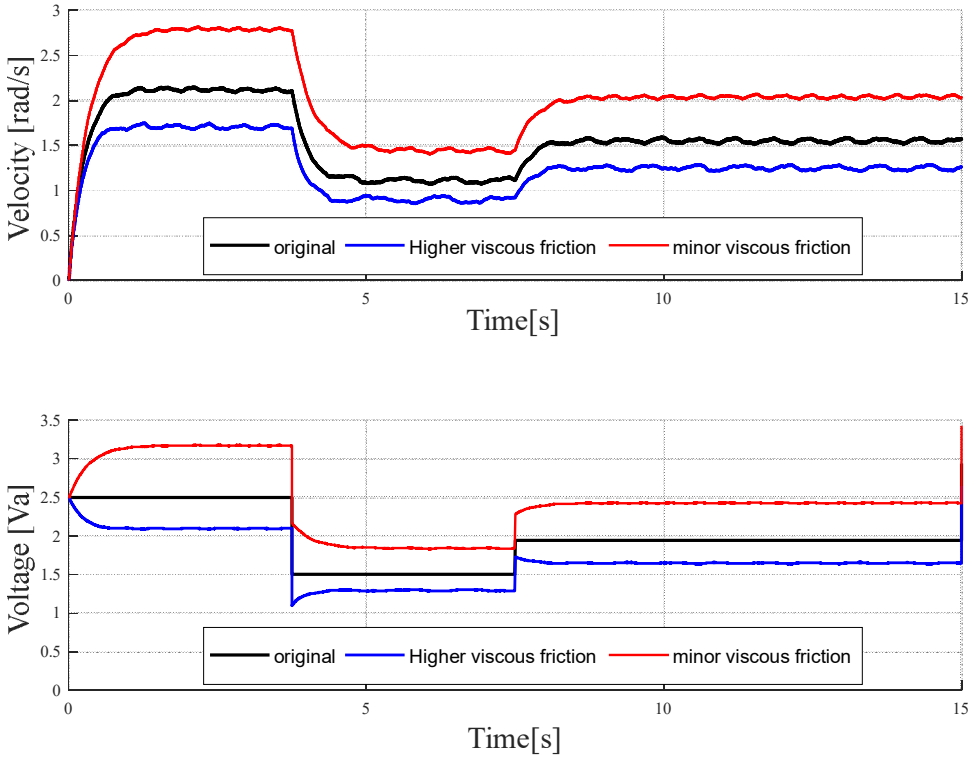

Figure 5. Velocity and control effort for ±25% changes in the coefficient of viscous friction and 100% in the friction of Coulomb.

Figure 6 show the plots of all involved variables of the mechanical impedance. These plots are related to the +25% change test in the apparent viscous friction where the final value changes can also be checked due to the proportional change of the gain in the first phase of the test.

4. DISCUSSION

Based on the performed experiments it was possible to notice that with only the increase of the apparent inertia, the armature voltage in the steady state does not change, but the system becomes slower during the transient response due to the apparent increase of the time constant, implying a possible degradation of the maneuverability. Maneuverability is considered here as the ability to make fast movements changes even with different velocities during the maneuver. By changing the apparent inertia to a value lower than nominal, the system shows a shorter time constant, allowing velocity variations to be imposed more quickly, increasing somehow system maneuverability. However, as the change in apparent inertia does not interfere with the final value of the response, the apparent viscous friction remains unchanged.

It was also possible to infer that, with a change in the coefficient of apparent viscous friction, the energy consumption to move the system also change. When the coefficient is changed further, it makes the transient response faster because of the apparent decrease in the time constant. The opposite is also true, that is, a decrease in the coefficient of apparent viscous friction, implies in higher steady-state velocity due to the assistance made by the motor, despite a slower transient.

Despite of the changes in apparent inertia and the apparent viscous friction coefficient, the Coulomb friction compensation also influences the system response. It is worth mentioning that the measured Coulomb friction is a global effect, that is, it includes belt friction, friction caused by motor brushes, etc. Applying the compensation of ±100% and ±50% of this friction, it is possible to identify a proportionality in the amplitude (gain). These gains cause the system to achieve higher speeds when controller compensates for friction. When the compensation adds friction to the system, the system reaches a lower speed.

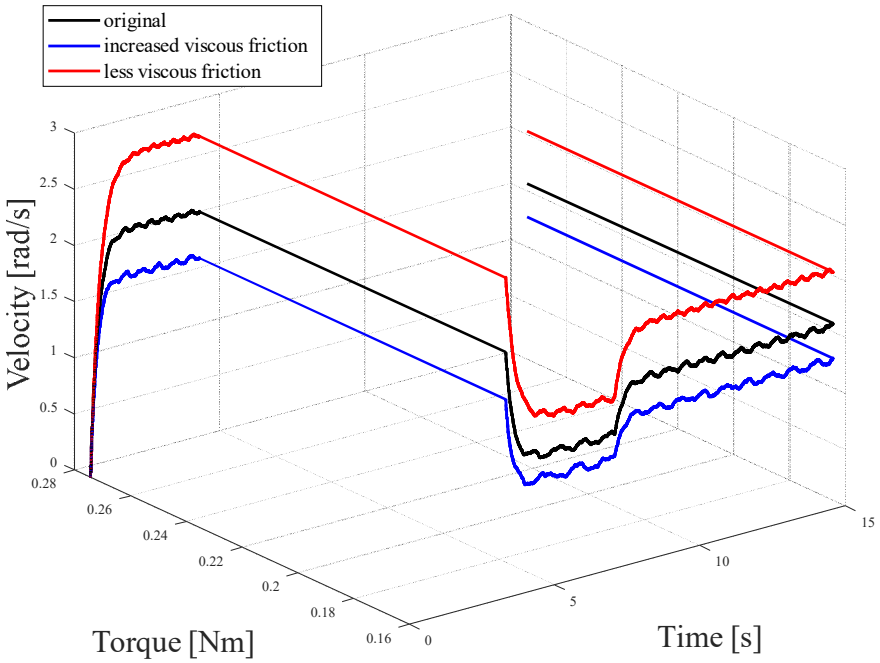

Figure 6. Mechanical impedance for + 25% changes in apparent viscous friction and -100% in Coulomb friction.

The proposed method allows changing the apparent parameters of the system, but it is necessary to select what is the appropriate set of parameter to apply for a particular application. There are different requirements for different situations such as when transporting loads in small spaces, requiring special care of the load and the environment, when the vehicle is in open spaces, or when the vehicle is on a slope.

According to Figure 7, it is possible to choose the range of parameters that can be used without the motor being outside of the working range, i.e. ±5 V. The solid of this figure was generated with the change from -95% to +95% for J_1, C_1, η_1 where the red part means region outside of the working range, so the values of that region cannot be used.

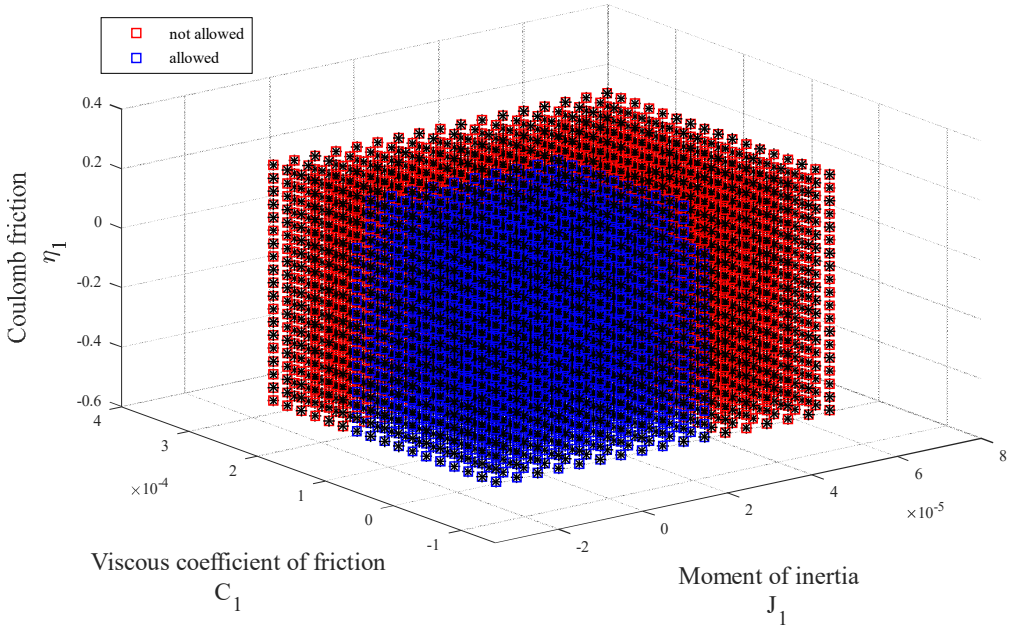

Figure 7. Range of parameters.

When the coefficient of viscous friction is lowered, the system will have a higher gain, thus the steady state of the velocity will be higher, which is of interest of the operator that will need to apply a smaller torque for the displacement.

In order to ensure safety when using the vehicle on slopes, the region with higher values of Coulomb friction, viscous friction, and with high moment of inertia should be used so that the velocity of the vehicle could be easily changed.

5. CONCLUSIONS

This work analyzed through numerical simulations and through experiments the performance of the impedance type control system for application in a cargo handling as a strategy for operator assistance.

The technique used was inspired by feedback linearization (calculated torque control) and was chosen because it does not need the use of force sensors. Because the control law does not process an impedance matching error, the control may present low robustness in the face of modeling errors. However, it was not an issue in our experiments.

The proposed control law allowed us change the apparent system impedance. The results observed in the simulations and in the experiments allow us to affirm that the mechanical impedance was imposed approximately as expected, even in the presence of unmodeled dynamics, such as inductance of the motor armature circuit and rigidities of the belts.

To validate the results, a load cell was also used to compare the impedance of the model with the actual impedance of the system. In this validation process, it was observed that for all imposed impedance, whose control effort was below the limit imposed by the saturation of the actuator, the experimental result was quite close to the values predicted by numerical simulation. The gain and the time constant presented variations proportional to the changes made, suggesting a good quality of the model.

As a proposal for the continuity of this research, it is suggested to investigate ways of defining a set of parameters that are more adequate for a given application. We suggest applying an optimization of the parameters, considering the saturation of the motor and the system maneuverability in the cost function. That is, the research could establish a criterion for choosing the apparent values of inertia, viscous friction and Coulomb friction

6. ACKNOWLEDGEMENTS

The authors would like to acknowledge Centro Universitário FEI and FAPESP (Fundação de Amparo à Pesquisa do Estado de São Paulo) for the research support.

7. REFERENCES

Arva, J., Fitzgerald, S.G., Cooper, R.A., Boninger, M.L., 2001 “Mechanical efficiency and user power requirement with a pushrim activated power-assisted wheelchair”. *Medical Engineering and Physics*, 23, 699-705.

Cooper, R.A., Corfman, T.A., Fitzgerald, S.G., Boninger, M.L., Spaeth, D.M., Ammer, W., Arva, J., 2002 “Performance Assessment of a Pushrim-Activated Power-Assisted Wheelchair Control System”. *IEEE Transactions on Control Systems Technology*, Vol. 10, No. 1.

Cuerva, V.I., Ackermann, M., Leonardi, F., 2016 “A Comparison of different assistance strategies in power assisted wheelchairs using an optimal control formulation”. In *Proceedings of the Modelling, Simulation and Identification IASTED. Campinas, São Paulo*, p. 97–102.

Dellabiancia, F., Porcellini, G., Merolla, G., 2013 “Instruments and techniques for the analysis of wheelchair propulsion and upper extremity involvement in patients with spinal cord injuries: current concept review”. *Muscles, ligaments and tendons journal,* 3 (3) 150-156.

Jardim, B., Martins, H.A., Siqueira, A.A.G., 2009 “Controle de Impedância Aplicado em uma Ortese Tornozelo-Pé Ativa”. In *Anais do 2º Encontro Nacional de Engenharia Bio-Mecânica. Florianópolis, SP*

Hogan, N., 1985 “Impedance control”. *Journal of Dynamic Systems, Measurement, and Control*, vol. 107, p.1-24.

Ibarra, J.C. P., Siqueira, A.A.G., 2014 “Impedance Control of Rehabilitation Robots for Lower Limbs”. In *Proceedings of the Conference on SBR-LARS Robotics Symposium and Robocontrol*.

Mehling, J.S., O’Malley, M.K., 2014 “A Model Matching Framework for the Synthesis of Series Elastic Actuator Impedance Control”. In *Proceedings of the* Mediterranean Conference on Control and Automation (MED) University of Palermo.

Pedro, L.M., Fernandes, G., Santos, W.M., Siqueira, A.A.G., Caurin, G.A.P., 2013 “Um estudo de desempenho do controle de impedância para tarefas de contato utilizando robôs industriais”. In *Anais do XI SBAI-Simpósio Brasileiro de Automação Inteligente. Fortaleza, Ceará Brasil*.

Popa, J., Liu, G., 2001 “Human Assisted Impedance Control of Overhead Cranes”. In *Proceedings of the International Conference on Control Aplication. Cidade do México.*

Sagawa Jr., Y., Haupenthal, A., Borges Jr, N.G., Santos, D.P., Watelain, E., 2012 “Wheelchairs propulsion analysis: review”. *Fisioterapia em movimento*, vol. 25.

Shibata, T., Murakami, T., 2012 "Power-Assist Control of Pushing Task by Repulsive Compliance Control in Electric Wheelchair". *IEEE Transaction on Industrial Electronics*, Vol.59, No.1.

Slotine, J.J., Li, W., 1991 *Applied Nonlinear Control*. Prentice-Hall

Rodriguez, O.M.H., Mudde, R.F., Oliemans, R.V.A., 2006. "Stability analysis of slightly-inclined stratified oil-water flow and intermediate wave theory". In *Proceedings of the 11th Brazilian Congress of Thermal Sciences and Engineering*. Curitiba, Brazil.

Trindade, M.A., Benjeddou, A., 2011a. "Finite element homogenization technique for the characterization of d15 shear piezoelectric macro-fibre composites". *Smart Materials and Structures*, Vol. 20, p. 075012.

Trindade, M.A., Benjeddou, A., 2011b. "Evaluation of effective material properties of thickness-shear piezoelec- tric macro-fibre composites". In *Proceedings of the 21st International Congress of Mechanical Engineering*. Natal, Brazil.

8. RESPONSIBILITY NOTICE

The authors are the only responsible for the printed material included in this paper.